



Open Access

ORIGINAL ARTICLE

Male Infertility

A recurrent homozygous missense mutation in *CCDC103* causes asthenoteratozoospermia due to disorganized dynein arms

Muhammad Zubair¹, Ranjha Khan¹, Ao Ma¹, Uzma Hameed², Mazhar Khan¹, Tanveer Abbas¹, Riaz Ahmad³, Jian-Teng Zhou¹, Wasim Shah¹, Ansar Hussain¹, Nisar Ahmed¹, Ihsan Khan¹, Khalid Khan¹, Yuan-Wei Zhang¹, Huan Zhang¹, Li-Min Wu¹, Qing-Hua Shi¹

Asthenoteratozoospermia is one of the most severe types of qualitative sperm defects. Most cases are due to mutations in genes encoding the components of sperm flagella, which have an ultrastructure similar to that of motile cilia. Coiled-coil domain containing 103 (*CCDC103*) is an outer dynein arm assembly factor, and pathogenic variants of *CCDC103* cause primary ciliary dyskinesia (PCD). However, whether *CCDC103* pathogenic variants cause severe asthenoteratozoospermia has yet to be determined. Whole-exome sequencing (WES) was performed for two individuals with nonsyndromic asthenoteratozoospermia in a consanguineous family. A homozygous *CCDC103* variant segregating recessively with an infertility phenotype was identified (ENST00000035776.2, c.461A>C, p.His154Pro). *CCDC103* p.His154Pro was previously reported as a high prevalence mutation causing PCD, though the reproductive phenotype of these PCD individuals is unknown. Transmission electron microscopy (TEM) of affected individuals' spermatozoa showed that the mid-piece was severely damaged with disorganized dynein arms, similar to the abnormal ultrastructure of respiratory ciliary of PCD individuals with the same mutation. Thus, our findings expand the phenotype spectrum of *CCDC103* p.His154Pro as a novel pathogenic gene for nonsyndromic asthenospermia.

Asian Journal of Andrology (2022) 24, 255–259; doi: 10.4103/aja2021122; published online: 04 March 2022

Keywords: asthenoteratozoospermia; *CCDC103*; dynein arms; male infertility

INTRODUCTION

The spermatozoa flagellum is an evolutionarily conserved organelle required for sperm mobility. It is composed of a microtubule-based structure named the “axoneme,” which comprises nine microtubule doublets (MTDs) and a central pair of microtubules (CPs).¹ The “axoneme” ultrastructure of sperm flagella is similar to that of motile cilia. Primary ciliary dyskinesia (PCD; Mendelian Inheritance in Man [MIM]: 244400) is a genetically heterogeneous autosomal recessive disorder caused by abnormalities of motile cilia such as bronchiectasis, respiratory infections, and situs inversus. Male infertility has also been reported in some PCD cases, and it is expected that genetic defects affecting motile cilia may have similar impacts on sperm flagella. To date, pathogenic mutations in more than 40 genes have been identified in PCD, yet only a few mutations have been reported to cause structural defects in sperm flagella in male individuals with PCD.² For example, mutations in the cilia and flagella associated protein 300 (*CFAP300*; Online Mendelian Inheritance in Man [OMIM]: 618058),³ dynein axonemal assembly factor 2 (*DNAAF2*; OMIM: 612517),⁴ leucine-rich repeat-containing 6 (*LRR6*; OMIM: 614930),⁵ and dynein axonemal intermediate chain 1 (*DNAI1*; OMIM: 604366)⁶ genes have been found

to cause an asthenospermia phenotype in male PCD patients. However, many mutations in PCD genes have unknown effects on male fertility, which may be due to two reasons: (1) there is a lack of routine semen analysis or sperm ultrastructure analysis of adult PCD male patients, and fertility assessment is rarely part of frontline PCD diagnostics; and (2) many PCD patients undergo genetic testing due to severe symptoms in childhood, and studies tracking the reproductive phenotype of these children into adulthood have not been performed.⁷

CCDC103, which is located on chromosome 7, is composed of four exons and encodes an oligomeric coiled-coil domain protein consisting of 242 amino acids (Q81W40-1).⁸ *CCDC103* is tightly bound to the ciliary axoneme and is vital for ciliary motility by participating in the attachment of the dynein arms to the axoneme. *CCDC103* loss-of-function mutations as well as the missense mutation p.His154Pro (rs145457535) were first identified in PCD patients with dynein arm loss in respiratory cilia.⁸ Later, the same mutation was found to be prevalent in the UK South Asian community. Respiratory cilia from p.His154Pro-mutated patients display different degrees of dynein arm defects, from a normal ultrastructure to partial outer and/or inner dynein arm defects.⁹ In addition, the p.His154Pro mutation has been

¹The First Affiliated Hospital of USTC, The CAS Key Laboratory of Innate Immunity and Chronic Diseases, School of Life Sciences, CAS Center for Excellence in Molecular Cell Science, Collaborative Innovation Center of Genetics and Development, University of Science and Technology of China, Hefei 230027, China; ²Institute of Industrial Biotechnology, Government College University, Lahore 54000, Pakistan; ³Medical Genetics Research Laboratory, Department of Biotechnology, Quaid-i-Azam University, Islamabad 45320, Pakistan.

Correspondence: Dr. LM Wu (wlm@ustc.edu.cn) or Dr. QH Shi (qshi@ustc.edu.cn)

Received: 03 August 2021; Accepted: 29 December 2021

functionally verified as a highly disruptive mutation that diminishes CCDC103 oligomerization ability.⁹ However, the affected individuals in these studies of CCDC103 were recruited from children's hospitals, and it is still unknown whether this highly recurrent CCDC103 missense mutation affects fertility.

In the present study, we recruited a consanguineous Pakistani family with two individuals with asthenoteratozoospermia and normal diagnostic results in PCD investigations. Whole-exome sequencing (WES) analysis identified the homozygous CCDC103 p.His154Pro mutation that was segregating recessively with an infertility phenotype. Transmission electron microscopy (TEM) of affected individuals' spermatozoa revealed a disordered axonemal ultrastructure and a complete lack of dynein arms (DAs). In summary, the results extend the phenotype spectrum of CCDC103 p.His154Pro to include causing nonsyndromic asthenoteratozoospermia.

PARTICIPANTS AND METHODS

Participants and clinical investigation

Two affected individuals (IV:1 and IV:7) with primary male infertility from a consanguineous family were recruited for this study (Figure 1a). A thorough questionnaire was completed by each participant covering his history of infertility. Both affected individuals had normal erection and ejaculation, and there were no signs or symptoms of PCD, according to clinical PCD investigations. Testicular diameters on both sides were normal, as was the development of male external genitalia and of secondary sexual traits. Tests for sperm concentration and motility were performed on the two affected individuals following the recommendations of the World Health Organization (WHO).¹⁰ For IV:1 and IV:7, sperm smear slides and sperm in TEM medium were obtained to evaluate sperm morphology and ultrastructural defects. Blood samples were collected from accessible family members. Written informed consent was obtained from all accessible family members.

The present study was approved by the Institutional Ethical Committee of the University of Science and Technology of China (USTC; Hefei, China) with the approval number of USTCEC202000003.

WES and bioinformatic analysis

The FlexiGene DNA kit was used to extract genomic DNA from peripheral blood samples according to the manufacturer's methodology (QIAGEN, Hilden, Germany). For WES, A1Exome Enrichment Kit V1 (iGeneTech, Beijing, China)-captured libraries were created for family members III:4, IV:1, IV:3, and IV:7 following the manufacturer's instructions. Sequencing was performed using the HiSeq 2000 platform (Illumina, San Diego, CA, USA). WES raw data processing was performed as previously reported,¹¹ and the detailed variant filtration pipeline is listed in **Supplementary Figure 1**. In addition, Sanger sequencing was performed for all participants (III:4, IV:1, IV:3, IV:5, and IV:7) using the primers of CCDC103 (forward: CTATCGTGATTGGCGACGAC, and reverse: AGACTGCTCCTCCAGACCCT; chr17: 42979771–42980122, 352 bp).

Sperm morphological analysis

In accordance with WHO standards,¹² all three patients had undergone routine semen analysis twice. Slides were sequentially immersed in 4% paraformaldehyde (PFA) for 5 min, washed with 1 × phosphate-buffered saline (PBS) twice for an additional 5 min, stained in hematoxylin (Solarbio, Beijing, China) for 30 min, dipped in purified water three times, immersed in 50% acidic ethanol, and kept in tap water for 2 min. The slides were dehydrated in 50% and 80% ethanol for 5 min each, stained for 5 min with Eosin Azure (Solarbio), sequentially dehydrated twice in 100% ethanol for 5 min each and in xylene for 5 min, and covered with coverslips with natural balsam. At least 300 stained spermatozoa per sample were analyzed by optical microscopy (Nikon, Tokyo, Japan).

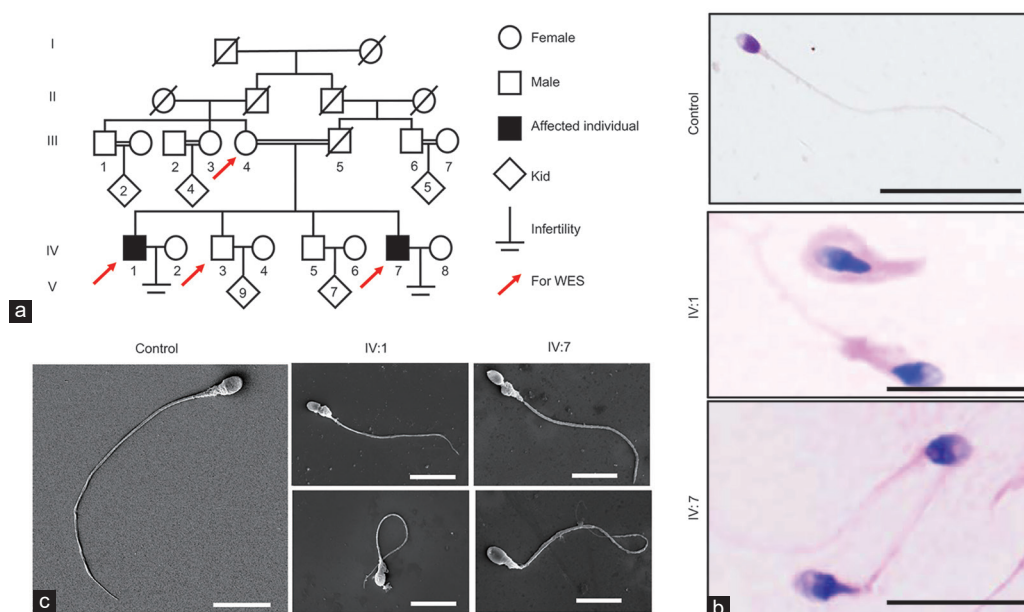


Figure 1: Two siblings with asthenoteratozoospermia in a Pakistani consanguineous family. (a) Two affected individuals (IV:1 and IV:7) with male infertility are the offspring of first-cousin marriage. Diamonds indicate a group of multiple progeny whose sex information was not available. Deceased family members are indicated with slash symbols. (b) Representative images of spermatozoa from fertile control and affected individuals (IV:1 and IV:7). Spermatozoa from the patients showed severe mid-piece and tail abnormalities. Scale bars = 50 μ m. (c) Representative spermatozoa images of scanning electron microscopy (SEM) from a fertile control and the affected individuals (IV:1 and IV:7). Spermatozoa from the patients showed swelled mid-pieces and coiled tails. Scale bars=10 μ m. WES: whole-exome sequencing.

Scanning electron microscopy (SEM) and TEM analyses

SEM and TEM analyses were carried out as we have previously described.¹³⁻¹⁵ Briefly, human spermatozoa were washed in PBS and then fixed overnight in 0.1 mol l⁻¹ cacodylate buffer (pH = 7.4) containing 0.2% picric acid, 4% paraformaldehyde, and 8% glutaraldehyde. For SEM, sperm were smeared onto a glass, followed by sequenced rinses and gradually dehydration. Then they were analyzed by Hitachi S-4800 Field Emission Scanning Electron Micro-scope (Hitachi, Tokyo, Japan) under an accelerating voltage of 15 kV. For TEM, selected spermatozoa were rinsed four times with 0.1 mol l⁻¹ cacodylate buffer and then fixed with 1% O₈O₄. These samples were subsequently dehydrated in 30%, 50%, 75%, 95%, and 100% ethanol and infiltrated with a mixture of acetone and resins. The samples were fixed in paraffin and sectioned into ultrathin sections (70 nm in thickness), after which they were stained with lead citrate and uranyl acetate. The flagellar ultrastructure was acquired and analyzed using a transmission electron microscope (Hitachi) operating at 100 kV or a microscope (Philips CM10, Philips Electronics, Eindhoven, The Netherlands) operating at 100 kV.

Immunofluorescence staining

Immunofluorescence of patient spermatozoa was performed as we have previously reported.¹³ Briefly, sperm from patients were smeared on clean slides and fixed with 4% paraformaldehyde followed by three washes in PBS. After permeabilization with 0.5% Triton X-100 for 30 min and blocking with 1% bovine serum albumin (BSA), the slides were incubated with primary antibodies, including anti- α -tubulin (F2168, Sigma, St. Louis, MO, USA), anti-dynein axonemal heavy chain 1 (anti-DNAH1; ab122367, Abcam, Cambridge, UK) and anti-dynein axonemal intermediate chain 2 (anti-DNAI2; ab171964, Abcam), overnight at 4°C. The next day, the slides were washed with PBS containing Triton X-100 (PBST) and incubated with secondary antibodies against donkey anti-rabbit-555 (DAR555; A31572, Molecular Probes, Eugene, OR, USA) and GAM488 (A21121, Molecular Probes) for 1 h at 37°C. Finally, the slides were washed again and sealed with Hoechst and Vectashield. Images were captured by using a laser scanning confocal microscope (Eclipse 80i, Nikon).

RESULTS

Clinical investigation of the patients

A Pakistani consanguineous family with two infertile brothers was selected for the current study (Figure 1a). Both affected individuals had a normal visceral position (Supplementary Figure 2); no symptoms of PCD were observed. Table 1 summarizes IV:1 and IV:7 sperm parameters and physical features. According to WHO recommendations,¹² both affected individuals had normal sperm counts (mean \pm standard error of the mean [s.e.m.]): IV:1 ($31.50 \times 10^6 \pm 4.95 \times 10^6$ ml⁻¹) and IV:7 ($26.50 \times 10^6 \pm 3.61 \times 10^6$ ml⁻¹). However, sperm motility (mean \pm s.e.m.) was very low: IV:1 ($4.5\% \pm 0.7\%$) and IV:7 ($4.0\% \pm 1.4\%$). To determine the possible reason for the severely compromised sperm motility, we analyzed sperm morphology in semen smear slides for IV:1 and IV:7. Typical abnormalities of sperm flagella, such as head and tail anomalies, were observed (Figure 1b). To study these anomalies in more detail, we carried out SEM of spermatozoa and detected swelled mid-pieces and coiled tails for both family members (Figure 1c). All these results indicate that IV:1 and IV:7 have asthenoteratozoospermia due to sperm flagellar defects.

WES identified a homozygous missense mutation in CCDC103

To identify the genetic cause of the defects in sperm flagella in this family, IV:1, IV:7, IV:3, and their mother III:4 were examined by WES. After a series of variant filtration steps, a CCDC103 homozygous

missense mutation (ENST00000035776.2, c.461A>C, p.His154Pro) was identified (Supplementary Figure 1). CCDC103 p.His154Pro was previously identified as a high-prevalence pathogenic mutation in PCD.^{8,9} Sanger sequencing for all available family members validated that this mutation was segregated recessively with an infertility phenotype (Figure 2).

Homozygous mutation p.His154Pro caused DA absence in patient spermatozoa

Since CCDC103 p.His154Pro has been reported to cause partial or total DA loss in respiratory ciliary tissue in PCD,^{8,9} we sought to explore whether the same ultrastructural defects might be found in IV:1 and IV:7 spermatozoa by TEM analysis, and 60 qualified cross-sections were analyzed for both affected individuals. In control samples, nine doublets of microtubules (DMTs) grouped circularly around the central pair complex (CPC; 9+2 organization) were observed in the axoneme structure. In contrast, more than 80% of sperm sections with a complete lack of DAs were observed for the affected brothers (Figure 3). To confirm the dynein anomalies, we performed immunostaining analysis for DNAI2 and DNAH1 antibodies (markers used to check assembly of outer dynein arms [ODA] and inner dynein arms [IDA]) on control and patient spermatozoa (Supplementary Figure 3a and 3b). We found intact and well-decorated signals of DNAI2 and DNAH1 on the whole tail of control spermatozoa. However, no specific signals were observed on the patient sperm, confirming the defective DA assembly. Altogether, the same severe DA abnormalities were observed in p.His154Pro-mutated spermatozoa as previously reported in p.His154Pro-mutated respiratory cilia.^{8,9}

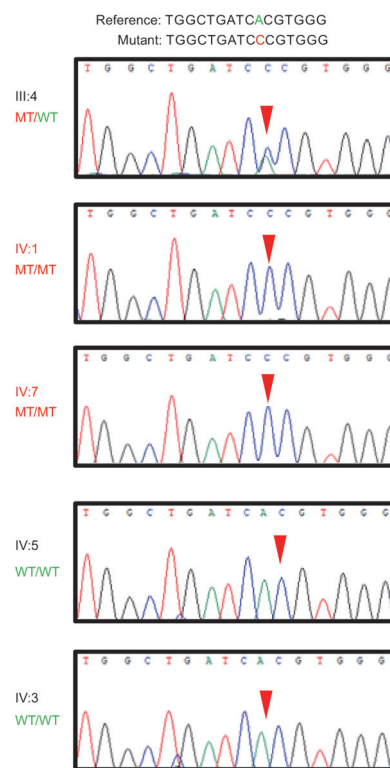


Figure 2: CCDC103 p.His154Pro cosegregated with an asthenoteratozoospermic phenotype in the pedigree. Sanger sequencing results revealed that CCDC103 p.His154Pro follows a recessive inheritance pattern. Mutation is indicated by red arrowheads in patients IV:1 and IV:7 (homozygous) and IV:3, IV:5, and III:4 (heterozygous). CCDC103: coiled-coil domain-containing 103; WT: wild type; MT: the mutation.

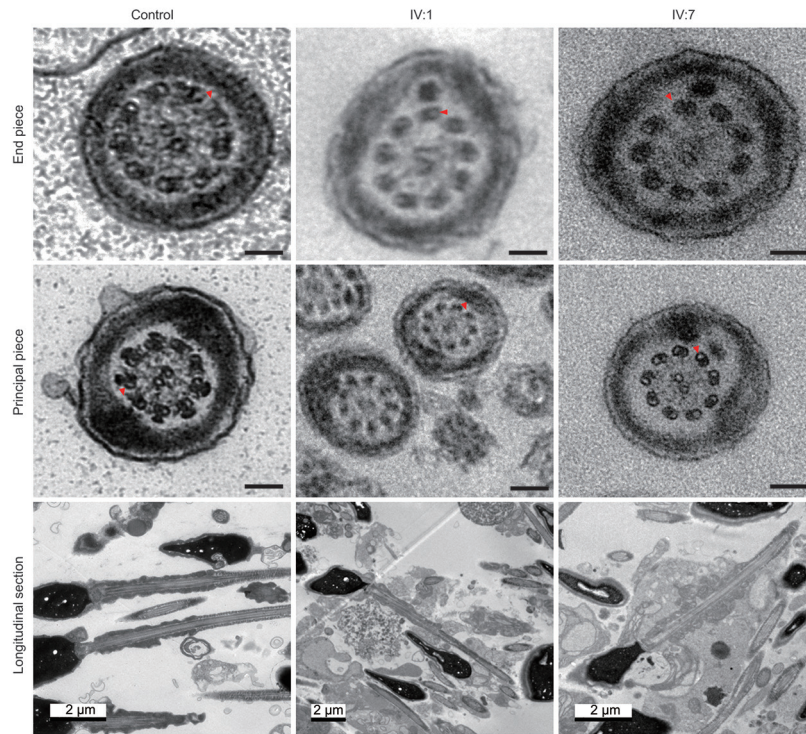


Figure 3: TEM analysis of *CCDC103* p.His154Pro spermatozoa revealed the absence of DAs. Representative TEM micrographs showing cross-sections of end piece (first line), middle principal piece (middle line), and longitudinal surface (bottom line) of sperm flagella from a fertile control (left part) and two patients (middle part IV:1 and right part IV:7). Scale bars = 2 μm. Red arrow indicates the normal DAs in control and the DA-absent place in patients. TEM: transmission electron microscopy; *CCDC103*: coiled-coil domain-containing 103; DA: dynein arm.

Table 1: Clinical characteristics of patients

Clinical characteristic	IV:1	IV:7
General information		
Fertility	Infertile	Infertile
Genotype	p.His154Pro/p.His154Pro	p.His154Pro/p.His154Pro
Age at diagnosis (year)	50	33
Height/weight (cm/kg)	158.0/79.0	161.6/89.0
Semen parameters		
Semen volume ^a (ml), mean±s.e.m.	3.25±1.06	3.50±1.00
Semen pH ^b	Alkaline	Alkaline
Sperm concentration ^c (×10 ⁶ ml ⁻¹), mean±s.e.m.	31.50±4.95	26.00±3.61
Normal sperm morphology ^d (%)	17.5±3.5	15.0±5.0
Active sperm (%)	4.5±0.7	4.0±1.4
Sluggish sperm (%)	14.5±0.7	6.3±1.5
Immotile sperm (%)	81.0±1.4	89.7±1.5
Flagellar defects (%)		
Coiled	40.0	36.8
Short	25.2	23.4
Bent	18.9	21.3
Multiple	7.4	6.3
Absent	4.2	6.7
Irregular caliber	1.1	1.4
Normal	3.2	4.1

Two independent experiments were performed. Reference values were published in WHO (2010): ^asemen volume >1.5 ml; ^bsemen pH is alkaline; ^csperm concentration >15×10⁶ ml⁻¹; and ^dnormal sperm morphology >4%. s.e.m.: standard error of mean; WHO: World Health Organization

DISCUSSION

Male infertility is an emerging issue that affects almost 12% of couples.¹⁶ One severe form of male infertility is due to lower progressive sperm motility.¹⁷ The flagellum is a sperm-specific organelle that is essential for motility.¹⁸ Both flagella and motile cilia have a conserved axonemal 9+2 microtubular arrangement. Therefore, pathogenic mutations in functional genes in motile cilia may also have an effect on sperm motility. In recent decades, with the development of next-generation sequencing techniques, genomic investigations of PCD have allowed for the identification of more than 40 genes whose mutations will cause PCD.² However, knowledge of the exact effects of PCD genes on sperm function is limited, either because of the lack of semen analysis in routine PCD clinical investigations or diagnosis in childhood. Therefore, the effect of PCD gene mutations on male fertility might be underestimated.

In the present study, we discovered the homozygous *CCDC103* p.His154Pro mutation in a Pakistani consanguineous family, with two infertile siblings with asthenoteratozoospermia. The *CCDC103* p.His154Pro variant was previously identified as a high-prevalence mutation in pediatric PCD patients, though without follow-up studies.^{8,9} Ultrastructural analysis of the spermatozoa of our patients showed that DAs were almost completely absent, which is similar to the most severe defect of *CCDC103* p.His154Pro-mutated respiratory cilia.

Pereira *et al.*¹⁹ first reported the *CCDC103* p.R35P variant in an infertile male patient who presented typical PCD symptoms, chronic respiratory complaints, and situs-inversus totalis. Later, the same group studied the effect of *CCDC103* p.R35P in nasal cells as well as in spermatozoa, and both kinds of cells showed a reduction in



CCDC103 mRNA expression and an absence of DA on axonemes.^{19,20} Unlike the patient carrying the CCDC103 p.R35P mutation, our patients did not display any typical PCD symptoms. This might be because the accuracy of PCD diagnosis requires strict clinical feature investigations, ultrastructural analysis of axonemes, motion analysis, and genetic testing.²¹

In previously reported childhood PCD cases with CCDC103 p.His154Pro mutations, the ultrastructure of the axoneme of respiratory cilia showed varying degrees of DA defects, ranging from apparently normal to complete ODA and IDA loss, which is consistent with impaired ciliary beating ability and respiratory symptoms. Patients with the same mutation but different phenotypic severities have also been found in another family with a CCDC103 loss-of-function mutation (p.Gly128fs25*).⁸ One child exhibited severe defects of both ODA and IDA, but other siblings with the same mutation had remnants of ODAs. The different degrees of phenotype severity observed among individuals carrying the same mutation suggests alteration of the phenotype by genetic modifiers, as is frequently observed in other autosomal recessively inherited disorders.²²

In our patients, CCDC103 p.His154Pro mutation appeared to lead to severe destruction of DAs in sperm flagella. However, combined with previous ultrastructural analysis of CCDC103 p.His154Pro-mutated respiratory cilia, the possibility remains that sperm flagella exhibit different degrees of ultrastructural abnormalities in patients with asthenospermia genetically diagnosed with CCDC103 p.His154Pro. For these cases, pathology-based PCD diagnostic protocols may provide a normal diagnosis, and further ultrastructural analysis of respiratory cilia, as well as close attention to patients who may present an unclear status or gradually develop PCD symptoms, is necessary. However, there is still a possibility that CCDC103 p.His154Pro only affects DA in sperm flagella in certain genetic backgrounds or that unknown genetic modifiers result in nonsyndromic male infertility. To cope with this issue, genetic testing for CCDC103 p.His154Pro is required in a larger asthenospermia cohort.

CONCLUSION

In conclusion, we report the CCDC103 p.His154Pro mutation with an asthenoteratozoospermia phenotype in a Pakistani consanguineous family, expanding the phenotypic spectrum of this mutation. These findings improve our understanding of sperm flagellar anomaly etiology and pathophysiology and provide further information for genetic counseling and diagnosis of both PCD and male infertility.

AUTHOR CONTRIBUTIONS

QHS and LMW conceived and designed the experiments. MZ, RK, and AM performed the experiments. MZ and JTZ analyzed the data. MZ and RK wrote the paper. TA, NA, KK, UH, MK, WS, AH, IK, YWZ, RA, HZ, and QS modified the manuscript. All authors read and approved the final manuscript.

COMPETING INTERESTS

All authors declare no competing interests.

ACKNOWLEDGMENTS

This work was supported by the National Natural Science Foundation of China (No. 81971446). We thank the Bioinformatics Center of the University of Science and Technology of China, School of Life Science, for providing supercomputing resources.

Supplementary Information is linked to the online version of the paper on the *Asian Journal of Andrology* website.

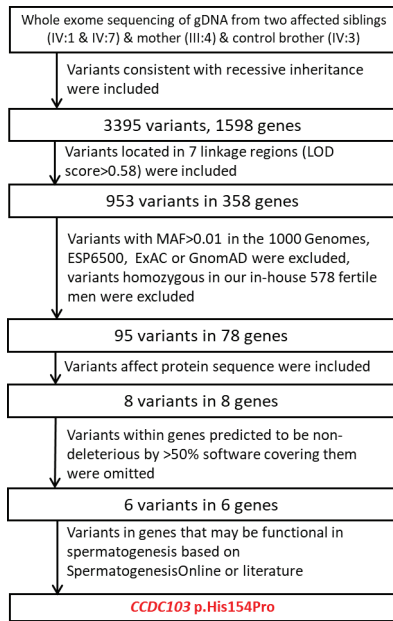
REFERENCES

- Inaba K. Molecular basis of sperm flagellar axonemes: structural and evolutionary aspects. *Ann N Y Acad Sci* 2007; 1101: 506–26.
- Sironen A, Shoemark A, Patel M, Loebinger MR, Mitchison HM. Sperm defects in primary ciliary dyskinesia and related causes of male infertility. *Cell Mol Life Sci* 2020; 77: 2029–48.
- Hoben IM, Hjeij R, Olbrich H, Dougherty GW, Nothe-Menchen T, *et al*. Mutations in *C11orf70* cause primary ciliary dyskinesia with randomization of left/right body asymmetry due to defects of outer and inner dynein arms. *Am J Hum Genet* 2018; 102: 973–84.
- Omran H, Kobayashi D, Olbrich H, Tsukahara T, Loges NT, *et al*. Ktu/PF13 is required for cytoplasmic pre-assembly of axonemal dyneins. *Nature* 2008; 456: 611–6.
- Kott E, Duquesnoy P, Copin B, Legendre M, Dastot-Le Moal F, *et al*. Loss-of-function mutations in *LRR6*, a gene essential for proper axonemal assembly of inner and outer dynein arms, cause primary ciliary dyskinesia. *Am J Hum Genet* 2012; 91: 958–64.
- Guichard C, Hricane MC, Lafitte JJ, Godard P, Zaegel M, *et al*. Axonemal dynein intermediate-chain gene (*DNAI1*) mutations result in situs inversus and primary ciliary dyskinesia (Kartagener syndrome). *Am J Hum Genet* 2001; 68: 1030–5.
- Goutaki M, Eich MO, Halbeisen FS, Barben J, Casaulta C, *et al*. The Swiss Primary Ciliary Dyskinesia registry: objectives, methods and first results. *Swiss Med Wkly* 2019; 149: w20004.
- Panizzi JR, Becker-Heck A, Castleman VH, Al-Mutairi DA, Liu Y, *et al*. CCDC103 mutations cause primary ciliary dyskinesia by disrupting assembly of ciliary dynein arms. *Nat Genet* 2012; 44: 714–9.
- Shoemark A, Moya E, Hirst RA, Patel MP, Robson EA, *et al*. High prevalence of CCDC103 p.His154Pro mutation causing primary ciliary dyskinesia disrupts protein oligomerisation and is associated with normal diagnostic investigations. *Thorax* 2018; 73: 157–66.
- Cao XW, Lin K, Li CY, Yuan CW. [A review of WHO Laboratory Manual for the Examination and Processing of Human Semen (5th edition)]. *Zhonghua Nan Ke Xue* 2011; 17: 1059–63. [Article in Chinese].
- Jiao Y, Fan S, Jabeen N, Zhang H, Khan R, *et al*. A *TOP6BL* mutation abolishes meiotic DNA double-strand break formation and causes human infertility. *Sci Bull* 2020; 65: 2120–9.
- World Health Organization. WHO Laboratory Manual for the Examination and Processing of Human Semen. 5th ed. Geneva: World Health Organization; 2010.
- Zhang B, Ma H, Khan T, Ma A, Li T, *et al*. A *DNAH17* missense variant causes flagella destabilization and asthenozoospermia. *J Exp Med* 2020; 217: e20182365.
- Zhang B, Khan I, Liu C, Ma A, Khan A, *et al*. Novel loss-of-function variants in *DNAH17* cause multiple morphological abnormalities of the sperm flagella in humans and mice. *Clin Genet* 2021; 99: 176–86.
- Khan I, Shah B, Dil S, Ullah N, Zhou JT, *et al*. Novel biallelic loss-of-function mutations in *CFAP43* cause multiple morphological abnormalities of the sperm flagellum in Pakistani families. *Asian J Androl* 2021; 23: 1–6.
- Choy JT, Eisenberg ML. Male infertility as a window to health. *Fertil Steril* 2018; 110: 810–4.
- Lehti MS, Sironen A. Formation and function of sperm tail structures in association with sperm motility defects. *Biol Reprod* 2017; 97: 522–36.
- Toure A, Martinez G, Kherraf ZE, Cazin C, Beurois J, *et al*. The genetic architecture of morphological abnormalities of the sperm tail. *Hum Genet* 2021; 140: 21–42.
- Pereira R, Oliveira J, Ferraz L, Barros A, Santos R, *et al*. Mutation analysis in patients with total sperm immotility. *J Assist Reprod Genet* 2015; 32: 893–902.
- Pereira R, Oliveira M, Santos R, Oliveira E, Barbosa T, *et al*. Characterization of CCDC103 expression profiles: further insights in primary ciliary dyskinesia and in human reproduction. *J Assist Reprod Gen* 2019; 36: 1683–700.
- Jackson CL, Behan L, Collins SA, Goggin PM, Adam EC, *et al*. Accuracy of diagnostic testing in primary ciliary dyskinesia. *Eur Respir J* 2016; 47: 837–48.
- Wirth B, Garbes L, Riessland M. How genetic modifiers influence the phenotype of spinal muscular atrophy and suggest future therapeutic approaches. *Curr Opin Genet Dev* 2013; 23: 330–8.

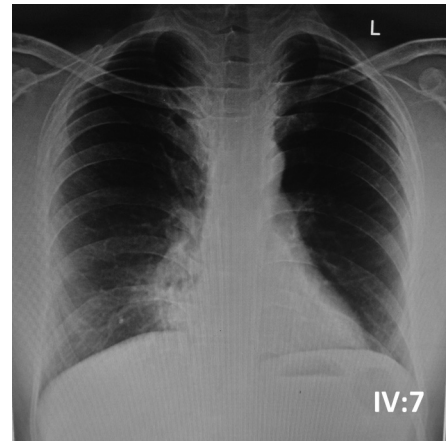
This is an open access journal, and articles are distributed under the terms of the Creative Commons Attribution-NonCommercial-ShareAlike 4.0 License, which allows others to remix, tweak, and build upon the work non-commercially, as long as appropriate credit is given and the new creations are licensed under the identical terms.

©The Author(s) (2022)

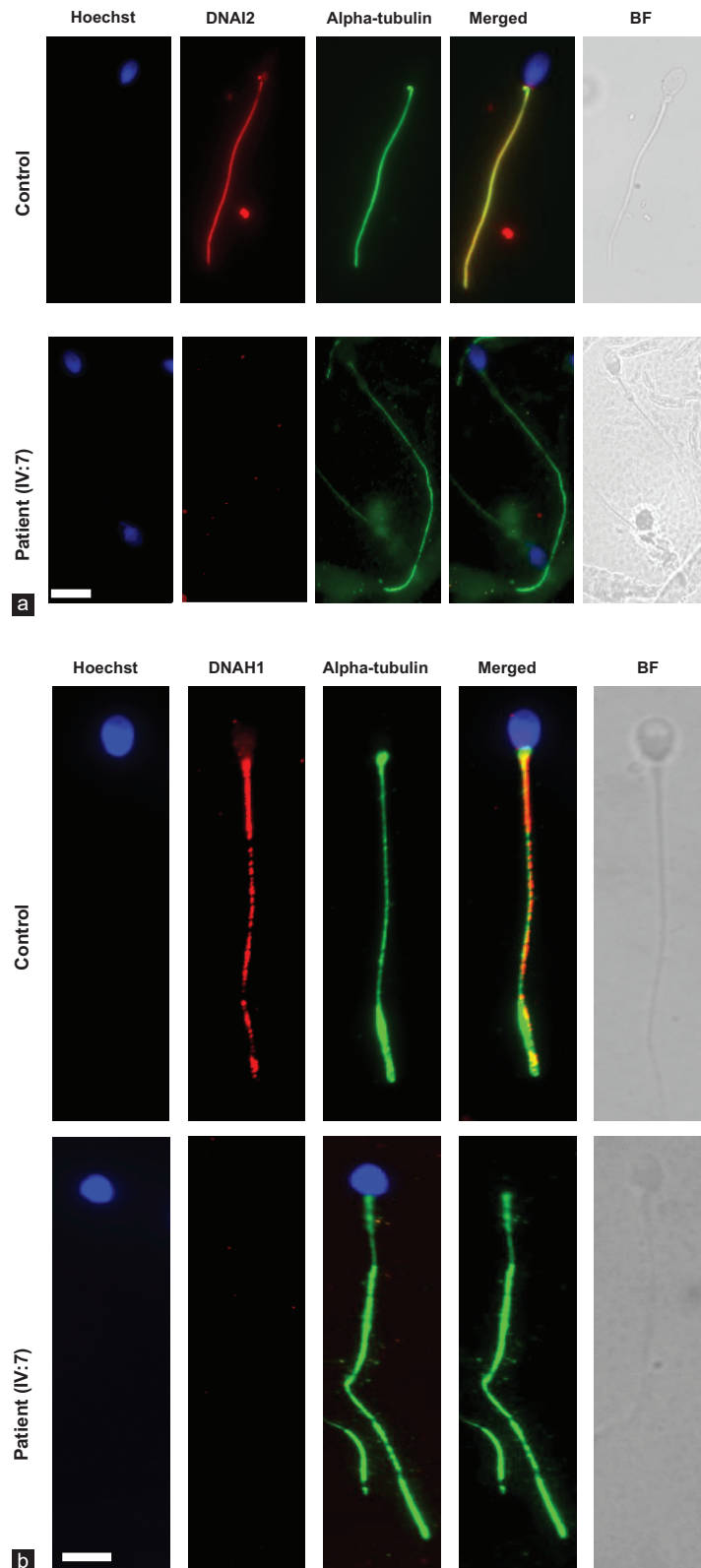




Supplementary Figure 1: WES data analysis flowchart. In the flowchart, variant filtration was performed using WES data from the two affected siblings (IV:1 and IV:7), a fertile brother (IV:3), and the mother (III:4). *CCDC103* p.His154Pro was identified as the candidate variant.



Supplementary Figure 2: X-ray clinical investigation. X-ray clinical study of IV:7 showed situs solitus.



Supplementary Figure 3: DNAI2 and DNAH1 immunostaining confirmed dynein arm disorganization. **(a)** Representative image of spermatozoa from fertile controls and patients stained with an anti-DNAI2 antibody, an anti- α -tubulin antibody, and Hoechst. Scale bars = 10 μ m. **(b)** Representative image of spermatozoa from fertile controls and patients stained with an anti-DNAH1 antibody, an anti- α -tubulin antibody, and Hoechst. Scale bars = 10 μ m.